PCCP

High-pressure-assisted X-ray-induced damage as a new route for chemical and structural synthesis

Journal:	*Physical Chemistry Chemical Physics*
Manuscript ID	CP-ART-04-2018-002119.R1
Article Type:	Paper
Date Submitted by the Author:	04-May-2018

Complete List of Authors:	Evlyukhin, Egor; University of Nevada Las Vegas, Physics and Astronomy Kim, Eunja; University of Nevada Las Vegas, Physics and Astronomy Goldberger, David; University of Nevada Las Vegas, Physics and Astronomy Cifligu, Petrika; University of Nevada Las Vegas, Physics and Astronomy Schyck, Sarah; University of Nevada Las Vegas, Physics and Astronomy Weck, Philippe; Sandia National Laboratories Pravica, Michael; University of Nevada Las Vegas, Physics and Astronomy

Journal Name

ARTICLE

High-pressure-assisted X-ray-induced damage as a new route for chemical and structural synthesis†

Received 00th January 20xx,
Accepted 00th January 20xx

DOI: 10.1039/x0xx00000x

www.rsc.org/

Egor Evlyukhin*[a], Eunja Kim[a], David Goldberger[a], Petrika Cifligu[a], Sarah Schyck[a], Philippe F. Weck[b], Michael Pravica[a].

X-ray induced damage has been known for decades and has largely been viewed as a tremendous nuisance. We, on the other hand, harness the highly ionizing and penetrating properties of hard X-rays to initiate novel decomposition and synthetic chemistry. Here, we show that powdered cesium oxalate monohydrate pressurized to ≤ 0.5 GPa and irradiated with X-rays of energies near the cesium K-edge undergoes molecular and structural transformations with one of the final products exhibiting a new type of *bcc* crystal structure which has previously not been observed. Additionally, based on cascades of ultrafast electronic relaxation steps triggered by the absorption of one X-ray photon, we propose a model explaining X-ray induced damage of multitype bounded matter. As X-rays are ubiquitous, these results yield promise to create novel compounds and novel structures that are inaccessible via conventional methods. They may offer insight into the formation of complex organic compounds in outer space.

Introduction.

Electronic excitation of atoms and molecules and subsequent relaxation processes are the main factors which cause X-ray induced radiation damage of matter.[1-6] Recent investigations of electronic decay processes induced by X-rays in loosely bound chemical systems demonstrated tremendous progress in understanding the sequence of events that leads to radiation induced damage.[1,7-11] Basically, absorption of a sufficiently energetic X-ray photon by an atom excites a K-shell electron to a bound state[2,3] or removes it from the host to the continuum[1] initiating a cascade of relaxation processes. The origin and sequence of relaxation processes strongly depend upon the chemical composition and environment of the irradiated system.[10,12-14] Recently, the role of metal ions in X-ray-induced photochemistry has been theoretically investigated.[1] It has been shown that absorption of X-rays by microsolvated Mg^{+2} results in cascade of ultrafast electronic relaxation steps that include both intra- and inter-molecular processes. At the end of this cascade, the metal ion reverts to its original oxidation state whereas the surrounding environment becomes multiply ionized and contains a many radicals and slow electrons. Such high capability of chemical systems to absorb X-ray photons which leads to distortion of molecular structure makes the study of these compounds using X-ray crystallographic techniques problematic. Thus, understanding the mechanisms of X-ray induced damage and the possibility to control this damage will be extremely useful for: (i) understanding the response of chemical systems to ionizing radiation, (ii) development of novel synthetic methods to create unique and potentially useful materials, and (iii) enabling more accurate analysis of their properties.

It should also be noted that complex molecules (including organic molecules) have been found in outer space[15] and many fundamental questions remain pertaining to how these compounds were synthesized over billions of years in or on comets, asteroids, or in the empty interstellar medium. Recently, we have demonstrated that X-rays with energies near the K-edge can be particularly effective in enabling chemical decomposition[16] and concomitant synthesis[6] including synthesis of a novel form of doped solid carbon monoxide.[17] As many biomolecules are polymers, one question that begs to be answered pertains to the probable role of X-rays in the synthesis of organic precursors (such as oxalate salts[18]) which may have themselves been delivered to the Earth and aided in the formation of living systems over integrated time.

In spite of accumulated knowledge mentioned above, the X-rays properties in terms of material synthesis are still unclear. Moreover little is known about the role of high pressure and radiation energy in X-ray induced photochemistry. In what follows we present an experimental study of the X-ray induced chemical and structural transformation of powdered cesium oxalate monohydrate ($Cs_2C_2H_2O_5$) at ambient and high pressure (≤ 0.5 GPa) by means of X-ray Diffraction (XRD). We found that X-rays assisted by high pressure open new reaction pathways via electronic excitation/ionization which differ from

[a] Department of Physics and Astronomy, University of Nevada Las Vegas (UNLV), 89154-4002 Las Vegas, Nevada, USA.
[b] Sandia National Laboratories, 87185 Albuquerque, New Mexico, USA Address here.
Electronic Supplementary Information (ESI) available.
See DOI: 10.1039/x0xx00000x

those activated by conventional methods[19] (i.e. high temperature and stoichiometric mixing) and drive the synthesis of novel materials with the formation of unique crystal structure properties. Additionally, we propose a model of X-ray induced photochemistry that demonstrates how X-ray photoabsorption by metal species triggers a cascade of electronic relaxation processes which results in multiple ionization of the surrounding environment, even in cases in which the metal reverts to its original charge state before the absorption of an X-ray photon.

Experimental methods.

All experiments were performed at the 16 BM-D beamline of the High Pressure Collaborative Access Team (HP-CAT) at the Advanced Photon Source. A tunable Si (111) double crystal in pseudo-channel-cut mode was used as a monochromator to filter "white" X-ray radiation and deliver X-rays of fixed but settable energies. A symmetric-style diamond anvil cell (DAC) with 250 µm thick stainless-steel gaskets was employed to confine and pressurize samples of powdered cesium oxalate monohydrate ($Cs_2C_2H_2O_5$). The diamonds utilized each had culets ~300 µm in diameter. All cesium oxalate ($Cs_2C_2O_4$) samples (Sigma-Aldrich, purity > 99%) were loaded inside a glove box into a ~140 µm diameter hole that was drilled via electric discharge machining in the gasket center that was pre-indented to ~40 µm thickness. Due to the high reactivity of $Cs_2C_2O_4$ with moisture all investigated samples contained water molecules and every sample was identified as $Cs_2C_2H_2O_5$. A ruby ball was loaded with each sample for pressure measurement purposes to ensure that the sample remained at ambient pressure or pressurized ≤ 0.5 GPa. No pressure-transmitting medium was used in the experiments. All samples were irradiated with X-rays ranging in energy from 30 to 42 keV for 40 min at each energy. The horizontal and vertical full width half-maximum (FWHM) of the X-ray beam varied from 3.5 - 4.2 µm as the energy of the beam changed. The corresponding photons flux varied from 3.31×10^7-1.13×10^7 ph/µm^{2}s as the energy of the beam changed from 30-42 keV (for 36keV the photons flux was 1.98×10^7 ph/µm^{2}s). Angular-dispersive X-ray diffraction patterns were collected every minute using a Pilatus®1M pixel array detector. We note that between each minute of X-ray irradiation there was a 1 min gap which is the time required for the software to transform and save collected data. The diffraction patterns were integrated in 2-theta using the Dioptas®program[20], to produce intensity versus 2-theta plots. Raman spectra of samples confined and compressed in DAC at room temperature were measured using an ISA HR460® spectrometer with a Peltier-cooled CCD detector (Andor® 1024x128 pixels). An Ar ion multiline laser tuned to 532 nm served as the excitation source.

Computational methods.

First-principles total energy calculations were performed using spin-polarized density functional theory (DFT), as implemented in the Vienna ab initio simulation package (VASP).[21] The exchange-correlation energy was calculated using the generalized gradient approximation (GGA), with the parametrization of Perdew, Burke, and Ernzerhof (PBE).[22,23] The interaction between valence electrons and ionic cores was described by the projector augmented wave (PAW) method.[24] The Kohn-Sham (KS) equation was solved using the blocked Davidson[25] iterative matrix diagonalization scheme followed by the residual vector minimization method. The plane-wave cut off energy for the electronic wavefunctions was set to a value of 500 eV, ensuring the total energy of the system to converge within 1 meV/atom. Electronic relaxation was performed with the conjugate gradient method accelerated using the Methfessel-Paxton Fermi-level smearing[26] with a Gaussian width of 0.1 eV. Ionic relaxation was carried out using the quasi-Newton method and the Hellmann-Feynman forces acting on atoms were calculated with a convergence tolerance set to 0.01 eV/Å. A periodic unit cell approach was used in the calculations. Structural relaxation was performed without symmetry constraints. The Brillouin zone was sampled using the Monkhorst-Pack k-point scheme[27] with 5×5×5 k-point meshes in all the calculations.

Results.

Samples of powdered $Cs_2C_2H_2O_5$ were loaded into DAC and

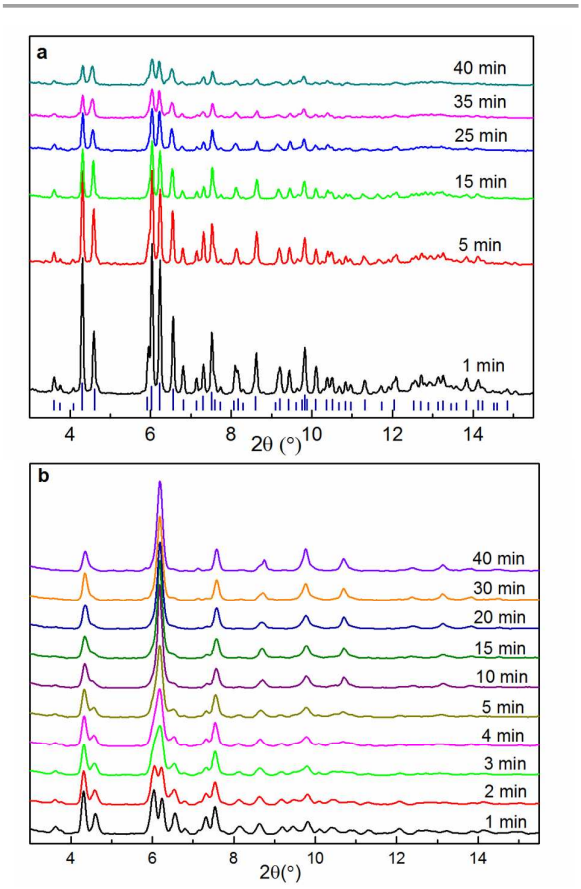

Fig.1. XRD patterns of cesium oxalate hydrate after different X-ray irradiation times. (a) $Cs_2C_2H_2O_5$ at ambient pressure; vertical bars indicate peak positions of the monoclinic crystal structure of cesium oxalate hydrate[29] (the full XRD pattern assignment is presented in Fig. S1 (ESI†)). (b) $Cs_2C_2H_2O_5$ at 0.3 GPa.

irradiated with monochromatic X-rays of selected energies, which were above or below the K-edge of cesium (35.987 keV)[28] at ambient and at high pressure (≤ 0.5 GPa). Fig. 1a displays *in situ* XRD patterns of $Cs_2C_2H_2O_5$ at ambient pressure after varying irradiation times using 36 keV X-rays.

The first XRD pattern after one minute of irradiation matches the previously reported monoclinic crystal structure of cesium oxalate hydrate[29] with *C2/c* space group (vertical bars in Fig. 1a). Upon further irradiation, the XRD peak intensities decrease indicating distortion of the electron density distribution (XRD patterns 5 - 40 min in Fig. 1a). Nevertheless, even after 40 min of X-ray irradiation, the XRD peak positions do not change and no new peaks are observed demonstrating that X-ray exposed $Cs_2C_2H_2O_5$ at ambient pressure does not undergo any structural transformations. On the other hand, the picture dramatically changes when high pressure is applied. Fig. 1b demonstrates the *in situ* XRD patterns of $Cs_2C_2H_2O_5$ at 0.3 GPa before and after different periods of X-ray irradiation at 36 keV. From the initial pattern (1min in Fig. 1b) recorded at 0.3 GPa, it is apparent that there is no pressure induced structural transformation due to its similarity with the ambient patterns presented in Fig. 1a. It is also evident from Fig. 1b that after 2 min of X-ray irradiation, the peak intensities significantly decrease whereas the peak positions remain the same. However, significant changes in the XRD pattern are observed immediately after the third minute of X-ray irradiation. Two peaks at 6.03° and 6.25° merge into one broad peak at 6.16°. Upon further irradiation up to 10 min, the XRD pattern changes completely. Many of the peaks observed in the initial XRD pattern disappear and a new peak forms at 10.71°. These dramatic changes indicate that irradiated $Cs_2C_2H_2O_5$ at 0.3 GPa undergoes a significant structural transformation. Continued X-ray irradiation up to 40 min does not modify the XRD pattern indicating that a major structural transformation occurs during the first 10 min of irradiation.

Our Raman spectroscopic studies indicated that after 40 min of X-ray irradiation at 0.3 GPa, the final product consists of different types of cesium-oxygen-based compounds[19,30-33] (See Fig. S2 (ESI†)). These are: cesium peroxide (Cs_2O_2)[19,30], cesium superoxide (CsO_2)[19,30-33] and cesium formate ($CHCsO_2$).[34] Based on these spectroscopic evidences, we performed first-principle calculations to identify the crystal structure of our final product. Fig. 2a displays an XRD pattern of the theoretically-predicted crystal structure of CsO_2, in comparison with an XRD pattern of our experimentally-derived product.

The excellent correspondence between experiment and theory verifies that at 0.3 GPa, the X-ray irradiated $Cs_2C_2H_2O_5$ largely transforms into CsO_2 with a new type of *bcc* crystal structure with space group *Pm-3m* (Z=1) and lattice parameter a = 4.5018 Å. Additional small peaks observed in our experimental data were found to be present in XRD patterns of Cs_2O_2 and $CHCsO_2$ crystal structures[35,36] (vertical bars in Fig. 2a) suggesting the slight present of these compounds in the final product. However, the predominance of CsO_2 in the obtained samples can be explained by its greater thermodynamic stability.[19] The uniqueness of the obtained crystal structure is

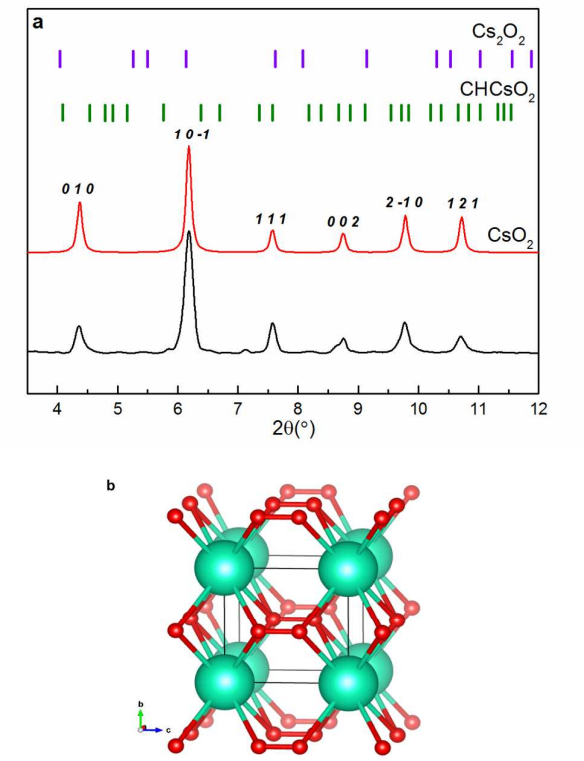

Fig.2. Characterization of structural properties of irradiated samples after 40 min of X-rays at 36 keV. (a) XRD patterns of the final product and theoretically predicted crystal structure of CsO_2 (diffraction peaks are labeled with Miller indices); vertical purple bars represent the orthorhombic crystal structure of cesium peroxide[35] with *Immm* space group and vertical green bars correspond to the orthorhombic crystal structure of cesium formate[36] with *Pbcm* space group. (b) Theoretically predicted crystal structure of CsO_2 with *Pm-3m* space group and the lattice parameter a = 4.5018 Å. Green and red spheres represent Cs and O atoms, respectively.

the unusual atomic positions within the unit cell. All Cs atoms are located in unit cell nodes whereas two oxygen atoms are inside the unit cell (see Fig. 2b) which is starkly different from the previously reported tetragonal (*I4/mmm*, Z=2) and cubic (*Fm-3m*, Z=4) crystal structures of cesium superoxide.[19,37,38]

Our DFT calculations indicate that the total energy differences between *Pm-3m* (Z=1), *I4/mmm* (Z=2), and *Fm-3m* (Z=4) are less than 0.1 eV/atom, while their simulated XRD patterns are clearly different (see Fig. S3 (ESI†)). We also note that oxides of cesium are typically low-work-function semiconductors which play a crucial role in engineering photoemissive devices[39] and in the promotion of catalytic reactions.[40] Therefore, we suspect that our final product with a unique crystal structure may be of significant technological interest.

The next question we address here pertains to the energy dependence of X-ray irradiation induced damage[6]. Samples of $Cs_2C_2H_2O_5$ pressurized in a DAC up to 0.3 GPa were irradiated with X-rays in the 32 - 42 keV energy range with 3 keV steps. After 40 min of irradiation at each energy, the same crystal

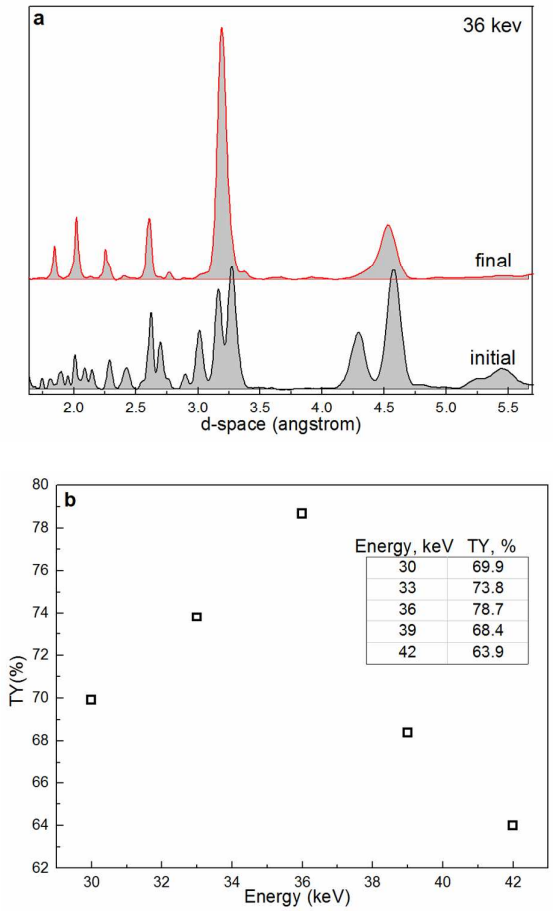

Fig.3. High-pressure assisted X-ray induced transformation yield (*TY*) of cesium oxalate hydrate. (a) Selected area (in grey) is presented in d-space (1.63 - 5.66 Å) plot of XRD patterns before (initial) and after 40 min (final) of X-ray irradiation of $Cs_2C_2H_2O_5$ at 0.3GPa. (b) X-ray induced *TY* of $Cs_2C_2H_2O_5$ at 0.3 GPa as a function of X-ray photon energy.

structure was obtained (see Fig. S4 (ESI†)) demonstrating that the structural transformation path does not depend upon the X-ray energy.

Nevertheless, to quantify X-ray induced structural transformations as a function of irradiation energy, we analyzed the change in integrated area underneath selected XRD peaks before and after irradiation. Fig. 3a demonstrates selected XRD peaks in d-space of $Cs_2C_2H_2O_5$ before and after 40 min of X-ray irradiation. The transformation yield (*TY*) as function of X-ray energy is defined as

$$TY = (Area_{final} \times 100\%) / Area_{int} \quad (1),$$

where $Area_{int}$ and $Area_{final}$ are respectively the integrated areas of selected peaks before and after 40 min of irradiation. The *TY* as a function of X-ray energy is presented in Fig. 3b. As seen in the figure, the maximum X-ray induced chemical and structural transformation (78.7 %) is achieved when the samples were irradiated at 36 keV, which is slightly above the K-edge of cesium (35.987 keV) suggesting that the energy of excited K-shell electrons plays an important role in X-ray induced damage. Indeed if the radiation energy is slightly above the K-edge of active species such as metal atoms the excited free electrons are slow and can be easily trapped by the neighboring atoms or molecules[34] resulting in multiple ionizations of the environment and subsequent dissociation.[1,7,10,42] As a result, the X-ray damaged system undergoes significant molecular and structural transformations.[17]

Discussion.

To better understand the nature of X-ray energy- and pressure-dependence of irradiation-induced damage discussed above, we propose a model of X-ray induced damage in multitype bounded matter. This model is based on previously reported studies of electronic relaxation processes triggered by X-ray absorption in weakly bound matter[1-3,7,10,11] and adapted for a chemical system which consists of strong (e.g. ionic) and weak (e.g. hydrogen) chemical bonds. The complex nature of ultrafast electronic relaxation steps triggered by X-ray photoabsorption that contain both intra- and intermolecular processes significantly complicates development of a mechanism to explain radiation induced damage triggered by multiphoton absorption. Therefore, here, we show that the radiation induced damage caused after the absorption of one X-ray photon by the metal cation can be essential even in cases when the metal ion reverts to its original charge state after photoabsorption.

Fig. 4 displays a proposed schematic representation of electronic decay processes triggered by absorption of one X-ray photon by a Cs atom with energies less than or equal to the energy of the cesium K-edge but higher than the cesium L-edge energy. Absorption of an X-ray photon by Cs excites its K-shell electron to a bound state[2,3] and initiates a cascade of relaxation steps. There are three possible decay processes which compete with each other depending on the ionization potential of created exited states[11]: (i) Auger decay[43] (typically dominant in metals) during which an electron with a characteristic energy is emitted by Cs^+ which, in turn, accumulates a positive charge: Cs^{+2}; (ii) intermolecular Coulombic decay (ICD)[44] when an excited cesium atom decays by transferring its excess energy only to a loosely bound water molecule[8] that would then emit a low-energy electron ($(H2O)^+$); and (iii) radiative decay during which the excited cesium atom decays via emission of characteristic X-rays (hv). After ICD or radiative decay, an excited cesium atom reverts to its original charge state, whereas Auger decay triggers additional cascades of relaxation steps to return Cs^{+2} to its initial Cs^+ charge state. These additional steps entail radiative decay and/or ICD[2,3] which are then followed by electron-transfer-mediated-decay (ETMD).[11] During ETMD, neighboring anions/molecules of $(C_2O_4)^{2-}$ or (H_2O) donate electrons to Cs^{+2} and the excess energy ionizes the donor itself (ETMD(1)), or another molecule (ETMD(2)). At the end of the ETMD steps, the cesium atom reverts to its original charge state and the surrounding environment is multiply ionized with a large concentration of slow electrons building up in the metal cation's vicinity.

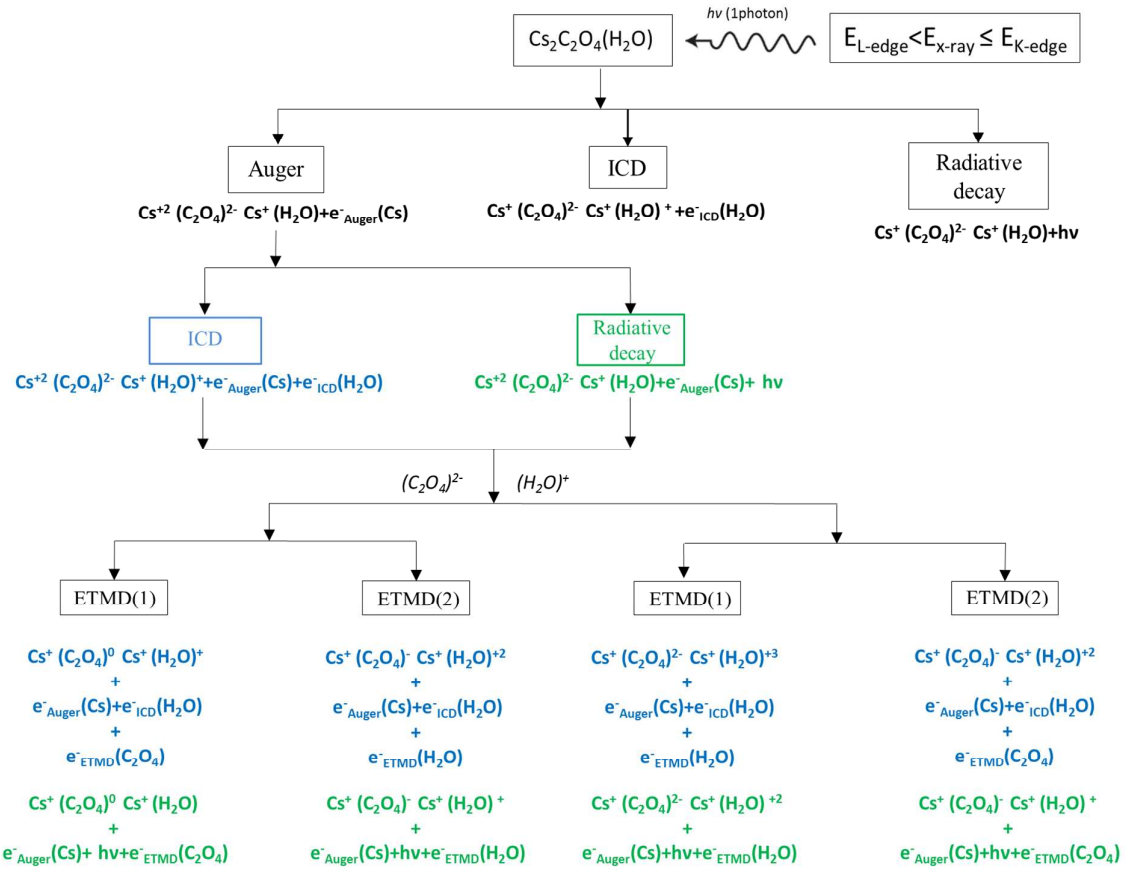

Fig.4. Schematic illustration of the electronic decay processes induced by absorption of one X-ray photon with energy less than K-edge of Cs but higher than the Cs L-edge by one $Cs_2C_2H_2O_5$ molecule. After each relaxation step, the changes of molecular oxidation states with the type of excited free electrons are presented. Different colors correspond to different relaxation paths.

The corresponding model changes when the energy of absorbed X-ray photon is above the cesium K-edge. Fig. 5 shows a proposed schematic representation of electronic decay processes triggered by absorption of one X-ray photon by a Cs atom with energies slightly (10-100 eV) or far (≥ 1 keV) above the cesium K-edge. In these cases, X-ray photon absorption by one Cs+ cation removes a core electron promoting it into the continuum.[1,43] During this process, the initial cesium charge state changes to Cs^{+2}. The created photoelectron may then secondarily ionize the surrounding environment depending on its energy[41]. The following chain of relaxation steps is similar to the previously discussed model with the exception of relaxation cascade paths followed after the first Auger decay. During Auger decay, an already ionized Cs^{+2} cation emits an electron with characteristic energies resulting in additional accumulation of positive charge (Cs^{+3}). After, three ETMD channels become possible: (i) a $(C_2O_4)^{2-}$ anion donates 2 electrons to Cs^{+3}; (ii) an H_2O molecule donates 2 electrons to Cs^{+3}; and (iii) a $(C_2O_4)^{2-}$ anion and (H_2O) molecule donate one electron each to Cs^{+3}. Depending on the neighboring electron donor, especially in cases when 2 electrons are donated to the metal ion, the excess energy is used to singly or doubly ionize the donor itself (ETMD (1)) or another molecule (ETMD(2)). As observed in Fig. 5, at the end of the electronic relaxation cascade, the metal surrounding environment is even more ionized than in the previous case ($E_{ph} \leq E_{K\text{-}edge}$) and contains a larger amount of released electrons, suggesting that X-ray photon energy plays an important role in radiation induced damage.

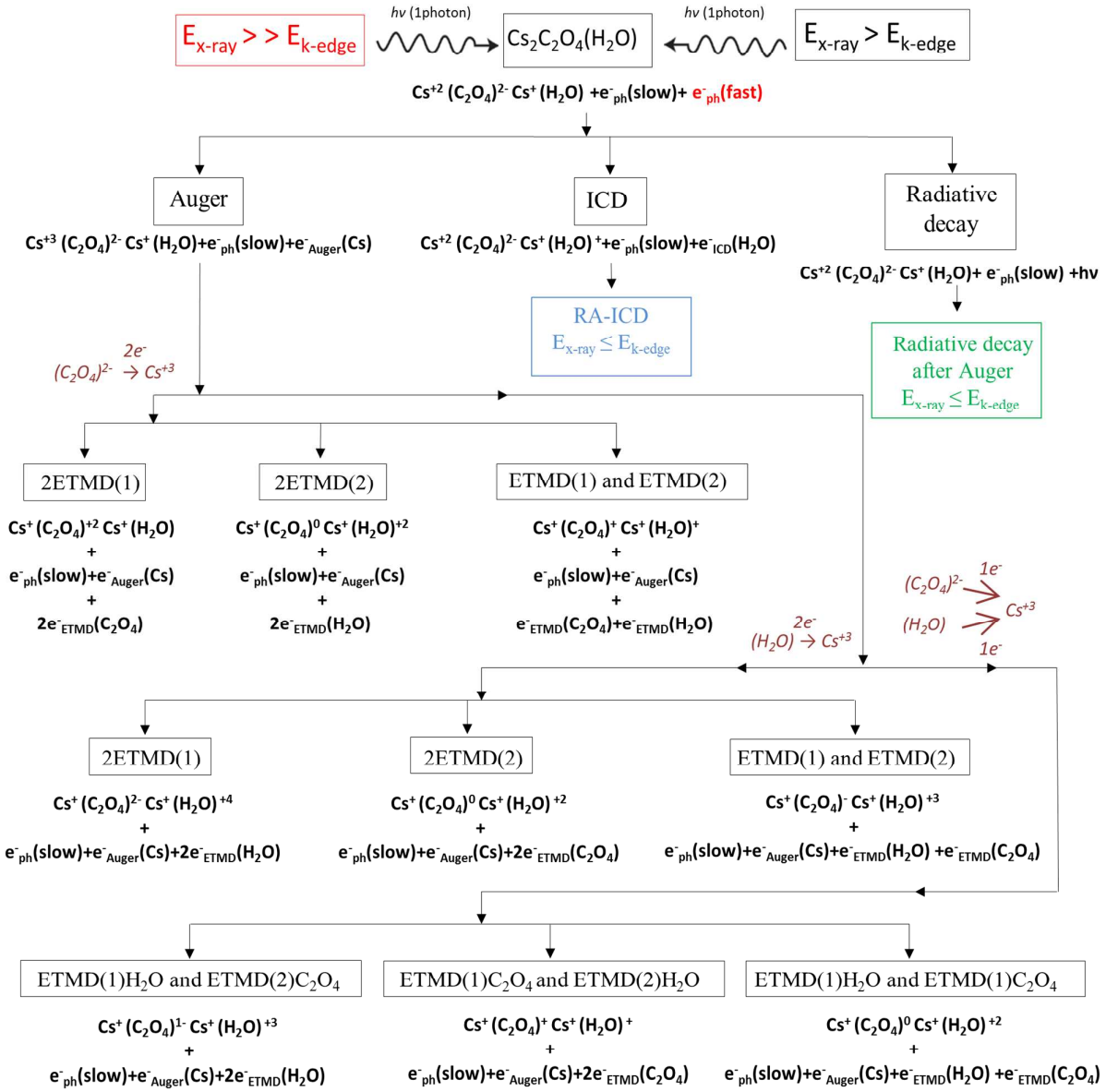

Fig.5. Schematic illustration of the electronic decay processes induced by absorption of one X-ray photon with energy slightly or far above the K-edge of Cs by one $Cs_2C_2H_2O_5$ molecule. After each relaxation step, the change of molecular oxidation states with the type of excited free electrons is presented. 2ETMD represents the relaxation process during which $(C_2O_4)^{2-}$ or $(H_2O)^{-}$ molecules donate two electrons to Cs^{+}. ETMD(x)A represent the relaxation process during which molecule A donates an electron to Cs^{+}, and the excess energy ionizes the donor itself (x=1) or another molecule (x=2).

Moreover, our experimental observation of an X-ray energy dependence of radiation induced damage may be supported by the proposed model. Indeed, we experimentally demonstrated that molecular and structural transformations induced by X-rays occur when investigated system is irradiated with photon energies both below and above the K-edge of metal species. Nevertheless, maximum transformation was achieved when samples were irradiated with energies slightly above the cesium K-edge at 36 keV. This can be explained by a larger concentration of slow electrons that have been produced in the metal's vicinity and which may then be trapped by the surrounding environment causing additional ionization[41]. This increases the possibility for molecular and structural transformations. Despite this myriad effects, X-ray induced structural transformations were only observed when high pressure was applied, suggesting that reduced inter-

molecular distance, even if molecules are ionized, is a necessary condition for the formation of a new crystalline structure. As discussed above, multiply ionized molecules will likely decompose[1,12,13] and, depending on the external conditions (pressure, temperature, irradiation), chemical reactions may proceed differently. We suspect that by pressurizing the sample, we have altered the free energy phase space for stable structures (local minima). Subsequently, irradiation with high energy X-rays enables the chemical system to overcome any activation barriers associated with accessing/creating these new structures.

Conclusions

In this work, we experimentally demonstrated that X-ray induced damage with high pressure assistance can be considered as a new route for material synthesis creating unique structures. We observed that $Cs_2C_2H_2O_5$ at pressure ≤ 0.5 GPa undergoes molecular and structural transformations even after 10 min of X-ray irradiation with energies less or above cesium K-edge. According to first-principle calculations, the crystal structure of the final product was identified as a new type of *bcc* crystal structure, which has not been previously reported to the best of our knowledge. These findings support our suggestion that *useful hard X-ray photochemistry* can be a potentially important tool for material synthesis.

Additionally, the energy dependence of X-ray induced molecular and structural transformation of $Cs_2C_2H_2O_5$ was interrogated. The maximum transformation yield (78.7 %) was achieved when the samples were irradiated at 36 keV, which is slightly above the K-edge of cesium (35.987 keV) suggesting that the excited K-shell electron energy plays an important role in the X-ray induced damage. These findings were also supported by a developed model, which explains the cascade of electronic relaxation processes triggered by X-ray photon absorption with different energies by the metal cation. We showed that even for cases when the metal ion reverts to its original charge state at the end of the relaxation cascade, the surrounding environment is multiply ionized with a large concentration of free electrons (with different energies). The ionized environment is highly unstable and intends to decompose according to the external conditions (pressure, temperature, and irradiation). We also note that prior investigations of X-ray induced damage of calcium (Ca)-DNA complex[45] and of iron-containing metalloenzymes4 observed that maximum damage occurred when samples were irradiated with X-rays at energies slightly above calcium and iron K-edges. Moreover, as living systems largely consist of complex organic molecules, some theories argue that some of these molecular precursors (such as oxalate salts and oxalic acid[18]) may have originated in outer space or on planetary surfaces (e.g. Mars) with an integrated dose of X-rays over many millions/billions of years. We feel that this study may provide us some insights into the mechanisms of formation of some important biologically-related systems within the deepest reaches of outer space.

Conflicts of interest

There are no conflicts to declare.

Acknowledgements

We gratefully acknowledge support from the Department of Energy National Nuclear Security Administration (DOE-NNSA) under Award Number DE-NA0002912. We also acknowledge support from the DOE Cooperative Agreement No. DE-FC08-01NV14049 with the University of Nevada, Las Vegas. Portions of this work were performed at HPCAT (Sector 16), Advanced Photon Source (APS), Argonne National Laboratory. HPCAT operation is supported by DOE-NNSA under Award No. DE-NA0001974, with partial instrumentation funding by NSF. The Advanced Photon Source is a U.S. Department of Energy (DOE) Office of Science User Facility operated for the DOE Office of Science by Argonne National Laboratory under Contract No. DE-AC02-06CH11357. Sandia National Laboratories is a multi-mission laboratory managed and operated by National Technology and Engineering Solutions of Sandia, LLC., a wholly owned subsidiary of Honeywell International, Inc., for the U.S. Department of Energy's National Nuclear Security.

References

1 V. Stumpf, K. Gokhberg, L. S. Cederbaum, The role of metal ions in X-ray-induced photochemistry, *Nature Chem*., 2016, **8**, 237-241.

2 K. Gokhberg, P. Kolorenč, A. I. Kuleff, L. S. Cederbaum, Site- and energy-selective slow-electron production through intermolecular Coulombic decay, *Nature*, 2013, **505**, 661-663.

3 F. Trinter, M. S. Schöffler, H. K. Kim, F. P. Sturm, K. Cole, N. Neumann, A. Vredenborg, J. Williams, I. Bocharova, R. Guillemin, M. Simon, A. Belkacem, A. L. Landers, T. Weber, H. Schmidt-Böcking, R. Dörner, T. Jahnke, Resonant Auger decay driving intermolecular Coulombic decay in molecular dimers, *Nature*, 2013, **505**, 664-666.

4 H. H. Jawad, D. E. Watt, Physical mechanism for inactivation of metallo-enzymes by characteristic X-rays, *Int. J. Radiat. Biol.*, 1986, **50**, 665-674.

5 O. Carugo, K. D. Carugo, When X-rays modify the protein struc-ture: radiation damage at work, *Trends Biochem. Sci.*, 2005, **30**, 213-219.

6 D. Goldberger, E. Evlyukhin, P. Cifligu, Y. Wang, M. Pravica, Measurement of the energy and high-pressure dependence of X-ray-induced decomposition of crystalline strontium oxalate, *J. Phys. Chem. A*, 2017, **121**, 7108-7113.

7 S. Thürmer, M. Ončák, N. Ottosson, R. Seidel, U. Hergenhahn, S. E. Bradforth, P. Slavíček, B. Winter, On the nature and origin of dicationic, charge-separated species formed in liquid water on X-ray irradiation, *Nature Chem*., 2013, **5**, 590-596.

8 L. S. Cederbaum, J. Zobeley, F. Tarantelli, Giant intermolecular decay and fragmentation of clusters, *Phys. Rev. Lett.*, 1997, **79**, 4778-4781.

9 T. Jahnke, Interatomic and intermolecular Coulombic decay: the coming of age story, *J. Phys. B: At. Mol. Opt. Phys*., 2015, **48**, 082001.

10 T. Jahnke, H. Sann, T. Havermeier, K. Kreidi, C. Stuck, M. Meckel, M. Schöffler N. Neumann, R. Wallauer, S. Voss, A. Czasch, O. Jagutzki, A. Malakzadeh, F. Afaneh, T. Weber, H.

Schmidt-Böcking, R. Dörner, Ultrafast energy transfer between water molecules, *Nature Phys.*, 2010, **6**, 139-142.
11 J. Zobeley, R. Santra, L. S. Cederbaum, Electronic decay in weakly bound heteroclusters: Energy transfer versus electron transfer, *J. Chem. Phys*., 2001, **115**, 5076-5088.
12 O. Marsalek, C. G. Elles, P. A. Pieniazek, E. Pluhařová, J. VandeVondele, S. E. Bradforth, P. Jungwirth, Chasing charge localization and chemical reactivity following photoionization in liquid water, *J. Chem. Phys*., 2011, **135**, 224510.
13 O. Svoboda, D. Hollas, M. Oncak, P. Slavicek, Reaction selectivity in an ionized water dimer: nonadiabatic ab initio dynamics simulations, *Phys. Chem. Chem. Phys*., 2013, **15**, 11531-11542.
14 P. E. Barran, N. R. Walker, A. J. Stace, Competitive charge transfer reactions in small $[Mg(H_2O)N]^{2+}$ clusters, *J. Chem. Phys*., 2000, **112**, 6173-6177.
15 B. A. McGuire, A. M. Burkhardt, S. Kalenskii, C. N. Shingledecker, A. J. Remijan, E. Herbst, M. C. McCarthy, Detection of the aromatic molecule benzonitrile (c-C_6H_5CN) in the interstellar medium, *Science*, 2018, **359**, 202-205.
16 M. Pravica, L. Bai, D. Sneed, C. Park, Measurement of the energy dependence of X-ray-induced decomposition of potassium chlorate, *J. Phys. Chem. A*, 2013, **117**, 2302-2306.
17 M. Pravica, E. Evlyukhin, P. Cifligu, B. Harris, J. Jae Koh, N. Chen, Y. Wang, X-ray induced synthesis of a novel material: Stable, doped solid CO at ambient conditions, *Chem. Phys. Lett.* 2017, **686**, 183-188.
18 D. M. Applin, M. R. M. Izawa, E. A. Cloutis, D. Goltz, J. R. Johnson, Oxalate minerals on Mars?, *Earth Planet. Sci. Lett*., 2015, 420, 127-139.
19 A. Band, A. Albu-Yaron, T. Livneh, H. Cohen, Y. Feldman, L. Shimon, R. Popovitz-Biro, V. Lyahovitskaya, R. Tenne, Characterization of oxides of cesium, *J. Phys. Chem. B*, 2004, **108**, 12360-12367.
20 C. Prescher, V. B. Prakapenka, DIOPTAS: a program for reduction of two-dimensional X-ray diffraction data and data exploration, *High. Press. Res*., 2015, **35**, 223-230.
21 G. Kresse, J. Furthmüller, Efficient iterative schemes for ab initio total-energy calculations using a plane-wave basis set, *Phys. Rev. B*, 1996, **54**, 11169-11186.
22 J. P. Perdew, J. A. Chevary, S. H. Vosko, K. A. Jackson, M. R. Pederson, D. J. Singh, C. Fiolhais, Atoms, molecules, solids, and surfaces: Applications of the generalized gradient approximation for exchange and correlation, *Phys. Rev. B*, 1992, **46**, 6671-6687.
23 J. P. Perdew, K. Burke, M. Ernzerhof, Generalized gradient approximation made simple, *Phys. Rev. Lett*., 1996, **77**, 3865-3868.
24 P. E. Blöchl, Projector augmented-wave method, *Phys. Rev. B*, 1994, **50**, 17953-17979.
25 E. R. Davidson, *Methods in Computational Molecular Physics,* Plenum: New York, 1983.
26 M. Methfessel, A. T. Paxton, High-precision sampling for Brillouin-zone integration in metals, *Phys. Rev. B*, 1989, **40**, 3616-3621.
27 H. J. Monkhorst, J. D. Pack, Special points for Brillouin-zone integrations, *Phys. Rev. B*, 1976, **13**, 5188-5192.
28 J. P. Gomilšek, A. Kodre, I. Arčon, M. Hribar, K-edge x-ray absorption spectra of Cs and Xe, *Phys. Rev. A*, 2003, **68**, 042505.
29 M. T. Weller, P. F. Henry, M. E. Light, Rapid structure determi-nation of the hydrogen-containing compound $Cs_2C_2O_4 \bullet H_2O$ by joint single-crystal X-ray and powder neutron diffraction, *Acta Crystallogr. B*, 2007, **63**, 426-432.
30 J. C. Evans, The peroxide-ion fundamental frequency, *J. Chem. Soc. D*, 1969, **0**, 682-683.
31 J. Li, R. J. Davis, Raman Spectroscopy and dioxygen adsorption on Cs-loaded zeolite catalysts for butene isomerization, *J. Phys. Chem. B*, 2005, **109**, 7141-7148.
32 K. R. Nemade, S.A. Waghuley, Synthesis of stable cesium superoxide nanoparticles for gas sensing application by solution-processed spray pyrolysis method, *Appl. Nanosci*., 2017, **7**, 753–758.
33 J. B. Bates, M. H. Brooker, G. E. Boyd, Raman spectra of O^{-2} and O^{-3} ions in alkali-metal superoxides and ozonides, *Chem. Phys. Lett*., 1972, **16**, 391-395.
34 K. Ito, H. J. Bernstein, The vibrational spectra of the formate, acetate, and oxalate ions, *Can. J. Chem*., 1956, **34**, 170-178.
35 H. Föppl, Die kristallstrukturen der alkaliperoxyde, *Z. Anorg. Allg. Chem*., 1957, **291**, 12-50.
36 M. P. Wilson, N. W. Alcock, P. M. Rodger, Structure of anhydrous alkali-metal formats, *Inorg. Chem*., 2006, **45**, 4359-4363.
37 V. Ya. Dudarev, A. B. Tsentsiper, M. S. Dobrolyubova, On phase transitions in rubidium and cesium epiperoxides, *Kristallografiya*, 1973, **18**, 759-763.
38 M. Ziegler, M. Rosenfeld, W. Kaenzig, P. Fischer, Strukturuntersuchungen an Alkalihyperoxiden, *Helv. Phys. Acta,* 1976, **49**, 57–90.
39 Y. Sun, Z. Liu, P. Pianetta, D-I. Lee, Formation of cesium peroxide and cesium superoxide on InP photocathode activated by cesium and oxygen, *J. Appl. Phys*., 2007, **102**, 074908.
40 R. J. Davis, New perspectives on basic zeolites as catalysts and catalyst supports, *J. Catal*., 2003, **216**, 396-405.
41 C. Müller, A. B. Voitkiv, J. R. C. López-Urrutia, Z. Harman, Strongly enhanced recombination via two-center electronic correlations, *Phys. Rev. Lett*., 2010, **104**, 233202.
42 B. Erk, R. Boll, S. Trippel, D. Anielski, L. Foucar, B. Rudek, S. W. Epp, R. Coffee, S. Carron, S. Schorb, K. R. Ferguson, M. Swiggers, J. D. Bozek, M. Simon, T. Marchenko, J. Küpper, I. Schlichting, J. Ullrich, C. Bostedt, D. Rolles, A. Rudenko, Imaging charge transfer in iodomethane upon x-ray photoabsorption, *Science*, 2014, **345**, 288-291.
43 R. W. Howell, Auger processes in the 21st century, *Int. J. Radiat. Biol*., 2008, **84**, 959-975.
44 T. Jahnke, A. Czasch, M. S. Schöffler, S. Schössler, A. Knapp, M. Käsz, J. Titze, C. Wimmer, K. Kreidi, R. E. Grisenti, A. Staudte, O. Jagutzki, U. Hergenhahn, H. Schmidt-Böcking, R. Dörner, Experimental observation of interatomic coulombic decay in neon dimers, *Phys. Rev. Lett*., 2004, **93**, 163401.
45 K. Takakura, Double-strand breaks in DNA induced by the K-Shell ionization of calcium atoms, *Acta Oncologica*, 1996, **35**, 883-888.

Graphical abstract

High-pressure-assisted X-ray-induced damage as a new route for chemical and structural synthesis.

Egor Evlyukhin[*†], Eunja Kim[†], David Goldberger[†], Petrika Cifligu[†], Sarah Schyck[†], Philippe F. Weck[‡], Michael Pravica[†].

[†]Department of Physics and Astronomy, University of Nevada Las Vegas (UNLV), 89154-4002 Las Vegas, Nevada, USA.

[‡]Sandia National Laboratories, 87185 Albuquerque, New Mexico, USA

A novel structural and chemical synthesis of Cs-O derived materials has been demonstrated via X-ray irradiation of $Cs_2C_2H_2O_5$ at high pressure.